

663757

DP-1203

AEC RESEARCH AND DEVELOPMENT REPORT

**^{238}U RESONANCE CAPTURE INTEGRALS FOR
RODS OF UO_2 , UC, AND U-METAL**

D. J. PELLARIN AND N. P. BAUMANN

RECORD COPY



Savannah River Laboratory

Aiken, South Carolina

SRL
RECORD COPY

LEGAL NOTICE

This report was prepared as an account of Government sponsored work. Neither the United States, nor the Commission, nor any person acting on behalf of the Commission:

A. Makes any warranty or representation, expressed or implied, with respect to the accuracy, completeness, or usefulness of the information contained in this report, or that the use of any information, apparatus, method, or process disclosed in this report may not infringe privately owned rights; or

B. Assumes any liabilities with respect to the use of, or for damages resulting from the use of any information, apparatus, method, or process disclosed in this report.

As used in the above, "person acting on behalf of the Commission" includes any employee or contractor of the Commission, or employee of such contractor, to the extent that such employee or contractor of the Commission, or employee of such contractor prepares, disseminates, or provides access to, any information pursuant to his employment or contract with the Commission, or his employment with such contractor.

Printed in the United States of America

Available from

Clearinghouse for Federal Scientific and Technical Information
National Bureau of Standards, U. S. Department of Commerce
Springfield, Virginia 22151

Price: Printed Copy \$3.00; Microfiche \$0.65

663757

DP-1203

Physics
(TID-4500, UC-34)

**^{238}U RESONANCE CAPTURE INTEGRALS FOR
RODS OF UO_2 , UC, AND U-METAL**

by

D. J. Pellarin and N. P. Baumann

Approved by

B. C. Rusche, Research Manager
Experimental Physics Division

January 1970

**E. I. DU PONT DE NEMOURS & COMPANY
SAVANNAH RIVER LABORATORY
AIKEN, S. C. 29801**

**CONTRACT AT(07-2)-1 WITH THE
UNITED STATES ATOMIC ENERGY COMMISSION**

ABSTRACT

Uranium-238 effective resonance capture integrals were measured in rods of UO_2 , UC, and U-metal. Rod diameters were 0.355, 0.500, 0.750, and 0.940 inch. Simultaneously activated thin foils of ^{238}U metal were the reference standards. The integrals included corrections for foil perturbation effects, counter efficiencies, and neutron spectra, which were determined from detailed measurements and computations. Analytical fits to the measured integrals, excluding the $1/v$ component, were $3.5 + 25.1 \sqrt{S/M_{\text{U}}}$ barns for U-metal, $5.25 + 24.35 \sqrt{S/M_{\text{UO}_2}}$ barns for UO_2 , and $5.05 + 26.2 \sqrt{S/M_{\text{UC}}}$ barns for UC, with S in cm^2 and M in grams. The integrals for the different chemical forms could not be correlated by any simple application of the equivalence theorem.

CONTENTS

	<u>Page</u>
List of Tables and Figures	4
Introduction	5
Experimental	5
Corrections	8
Non-1/E Epithermal Flux Spectrum	8
Counting Corrections	12
Deadtime	12
Fission Products	12
Foil Size - Counter Efficiency	12
Correction for $RI^{1/v}$ Component	12
Resonance Shielding Correction	13
Finite Length Rod Correction	14
Foil Gap Correction	16
Correction for Use of Metal Foils in UO_2 and UC Rods	18
Radial Misalignment of Foils	19
Results	21
References	25

LIST OF TABLES AND FIGURES

<u>Table</u>		<u>Page</u>
I	Uranium Metal Resonance Integrals Measured in SP and PDP	11
II	Uranium Metal Resonance Integral Results - Rods . .	21
III	Uranium Metal Resonance Integral Results - 0.500-inch-Diameter Foil Packets	21
IV	Uranium Oxide Resonance Integral Results - Rods . .	23
V	Uranium Carbide Resonance Integral Results - Rods .	24

<u>Figure</u>		
1	Test Apparatus	6
2	Monte Carlo Computed Epithermal Flux Spectrum in SP	9
3	Monte Carlo Computed Resonance Integral Ratios Compared to Experimental Activation Ratios	10
4	Monte Carlo Computed Epithermal Flux Spectrum in SP and PDP	11
5	Comparison of Computed and Measured Finite Length Rod Corrections	15
6	Geometrical Model for Computing Effect of Gaps at Measuring Foils on Resonance Integral	16
7	Comparison of Computed and Measured Gap Corrections	17
8	Models Used to Determine Uranium Metal Foil Perturbation in UO ₂ Rods	18
9	Effect of Radial Misalignment on Foil Activities in 0.500-in.-Diameter Uranium Metal Bar	20
10	Effective Resonance Integral for Uranium Metal . .	22
11	Effective Resonance Integrals for UO ₂ and Equivalence Theorem Comparison	23
12	Measured Uranium Carbide Resonance Integrals and Equivalence Theorem Comparison to Uranium Metal . .	24

INTRODUCTION

The resonance integral for ^{238}U capture is an important parameter in the design and analysis of thermal reactors fueled with natural uranium. Despite a number of careful studies,^{1,2} the effective resonance integrals found for uranium metal rods still disagree outside their quoted errors. This report gives effective ^{238}U neutron capture integrals of uranium metal, dioxide, and monocarbide rods of various diameters that include significant alterations not made in earlier measurements. These alterations include an extension of the surface-to-mass range of the U-metal measurements, careful consideration of the actual resonance flux energy spectrum, and detailed investigations of corrections to various experimental variables. The integrals were determined by the cadmium ratio-activation method. The dilute resonance integral of gold³ (RI = 1490 \pm 40 barns) served as the primary standard.

EXPERIMENTAL

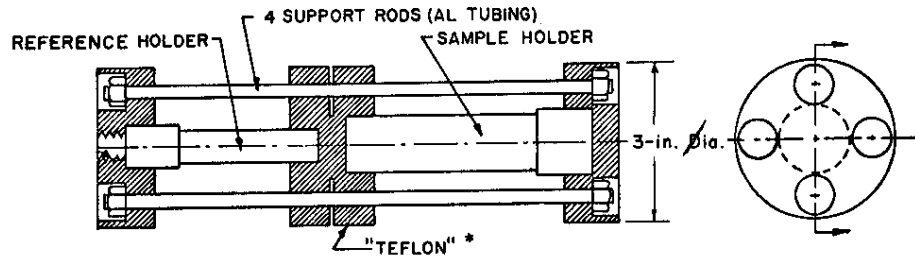
The resonance integral measurements were made in the 3.00-inch-diameter central axis irradiation port of the Standard Pile⁴ (SP) at the Savannah River Laboratory (SRL). The SP is a 5-foot cube of graphite containing an annular core loaded with fuel discs of fully enriched uranium and filled with H_2O . At the irradiation position near the center of the SP, the epithermal neutron flux spectrum is closely proportional to $1/E$ from 1 ev to 2 kev. Above 2 kev the spectrum exceeds $1/E$.

The test apparatus (Figure 1) consisted of two aluminum cylinders (holders) covered by 32 mils of cadmium sheathing and rigidly held in a "Teflon"* and aluminum rod assembly. The measurements were made by simultaneously irradiating a 0.002-inch-thick depleted (0.19% ^{235}U) uranium sample foil in a rod section [or an assembled packet of 0.500-inch-diameter, 0.002-inch-thick depleted (0.19% ^{235}U) uranium foils] located inside the larger sample holder and an identical 0.500-inch-diameter foil in the smaller reference holder.

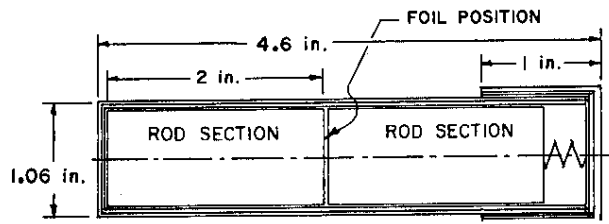
The effective resonance integral for the sample foil(s) was calculated (after appropriate corrections to be discussed later) by

$$RI_S^{\text{eff}} = \frac{(\text{Act})_S}{(\text{Act})_R} \times \frac{\phi_R^{\text{epi}}}{\phi_S^{\text{epi}}} \times RI_R^{\text{eff}}$$

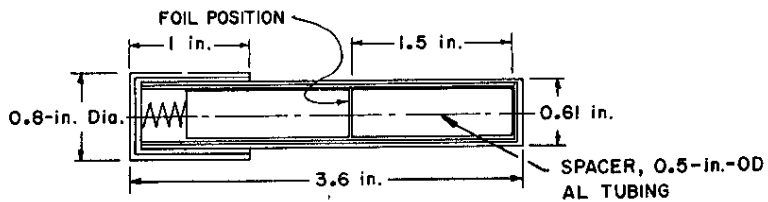
* Du Pont's trademark for its fluorocarbon plastic.



ASSEMBLED TEST APPARATUS



SAMPLE HOLDER



REFERENCE HOLDER

* DuPont Trademark

NOTE: BOTH HOLDERS MADE OF 0.020 in. AL AND CLAD WITH 0.032 in. Cd

FIG. 1 TEST APPARATUS

where the subscripts S and R refer to the sample and reference foils, respectively. The ratio of the incident epithermal fluxes $\phi_R^{epi}/\phi_S^{epi}$ was obtained from separate flux calibration experiments using an isolated foil in the sample holder. The ratio of the specific activations $(Act)_S/(Act)_R$ was determined by counting the 2.3-day decay of ^{239}Np in a 90 to 116 keV window of a NaI scintillation spectrometer. The foils were counted in the interval from 2 to 4 days following irradiation because this timing minimized the fission product background and the counter deadtime corrections. The effective resonance integral of the reference foil RI_R^{eff} was obtained from the expression by Hellstrand,¹ $RI^{eff} = 4.05 + 25.1 \sqrt{S/M_U}$ barns, with S in cm^2 and M in grams. This expression had been used in a previous study⁵ to represent the effective resonance integral for the reference foils. In that study, effective resonance integrals for ^{238}U had been determined for $\sqrt{S/M}$ values of 1.54 to 200 $\text{cm/g}^{1/2}$ (infinite dilution) by the cadmium ratio-activation technique using the dilute resonance integral of gold as the standard. The experiment had been performed by irradiating the foils on a spinner apparatus located near the center of the SP. The Hellstrand expression had been found to fit the measurements precisely for $\sqrt{S/M}$ values of 1.5 to 5.5 $\text{cm/g}^{1/2}$.

Integrals were determined for natural U-metal rods 4 inches long, natural UO_2 rods 4 inches long, and UC rods <4 inches long with diameters of 0.940, 0.750, 0.500, and 0.355 inch. Integrals were also determined for U-metal with an S/M range intermediate between rods and individual foils by assembling 0.500-inch-diameter foils into packets of various length, irradiating the packet in the sample holder, and determining the average specific activation of the packet by counting the individual foils. The S/M value for each packet was determined from the dimensions and weight of the assembled packet.

CORRECTIONS

Non-1/E Epithermal Flux Spectrum

The definition of a resonance integral is based on a neutron energy distribution that varies as $1/E$. Any departure from a $1/E$ flux spectrum produces an error component in the measured resonance integral. The percentage error is largest for small $\sqrt{S/M}$ values. Earlier measurements of resonance integrals in the center of the SP had indicated that the epithermal flux spectrum is closely $1/E$ from 1 ev to 2 kev.⁵ The spectrum at higher energies was computed using the CASINO Monte Carlo code.⁶ The following assumptions were made in adapting and applying the code to the SP:

- a) The reactor is infinitely long in the axial direction, i.e., there is no axial leakage.
- b) The axial reflector is an extension of the core region.
- c) The annular core, made up of H_2O , aluminum, and ^{235}U , can be homogenized on a volume weighted basis.
- d) The infinite length, square, parallelepiped model assumed for the SP can be replaced by an equivalent cylindrical model that preserves the geometrical buckling.

Because the limitations of the code require that the source neutrons be introduced in only one discrete location in the fuel region, a run was made for each of three different source locations. The functional shape of the true source distribution was obtained by a separate diffusion theory calculation using slab geometry, and the spectrum for the distributed source was obtained by graphical and numerical integration of the separate discrete source spectra. Figure 2 shows the computed epithermal flux spectrum for each region in the SP. The spectra are normalized at 4.9 ev which corresponds to the dominant resonance of gold which was used as the primary standard. The coarse geometrical grid structure, shown in detail in Figure 2, was necessary to obtain good statistics. The strong flux peaking at high energies in the graphite region indicates that a significant fraction of the fission neutrons reach the core with little or no energy loss.

The computed flux spectrum in the SP was experimentally confirmed by using the spectrum to calculate the resonance integral ratio between a 0.500-inch-diameter, 2-mil-thick U-metal foil and a 0.500-inch-diameter, infinite length U-metal rod, and then comparing the ratio to a measurement of the corresponding activation ratio. The activation ratio is sensitive to the flux spectrum

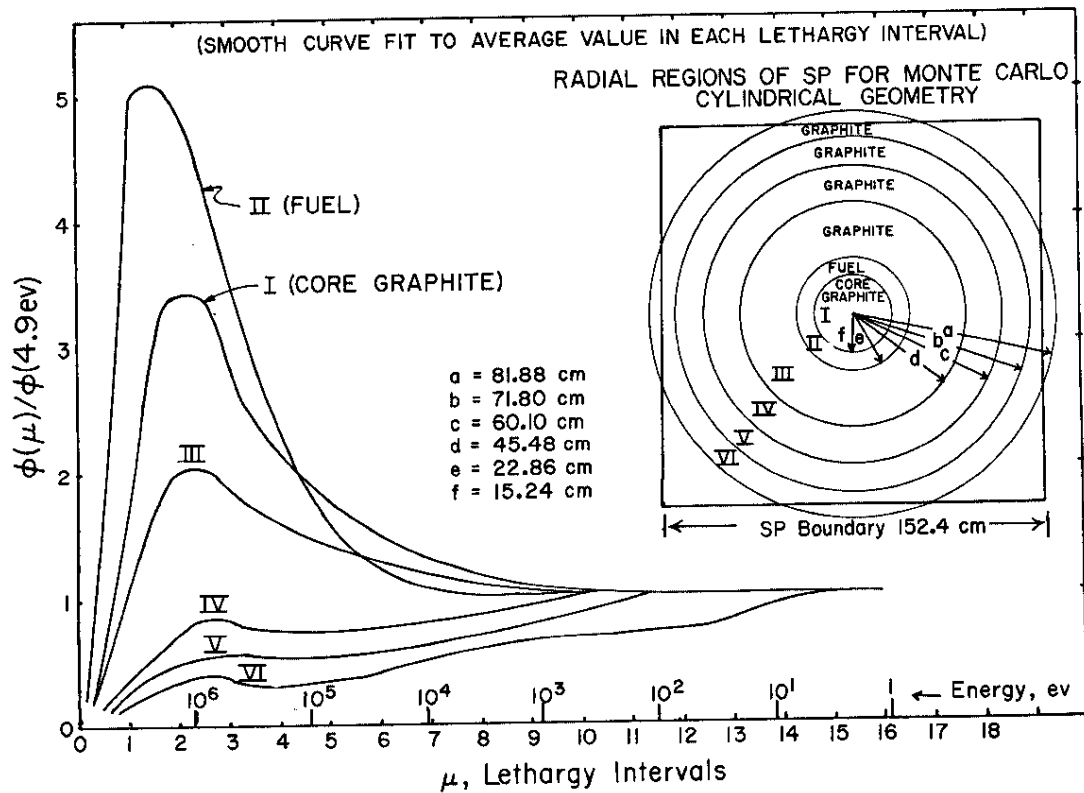


FIG. 2 MONTE CARLO COMPUTED EPITHERMAL FLUX SPECTRUM IN SP

because the foil is preferentially activated by low energy neutrons, and the rod by higher energy neutrons. The calculation and measurement were made at several radial locations in the SP. To calculate the ^{238}U capture at each location, the effective ^{238}U resonance capture integrals used for the foil and the rod had to be divided into small lethargy intervals. Therefore, above 10 kev, the BNL⁷ directly measured cross sections were used; from 1 to 10 kev, Vernon's⁸ shielded cross sections were used; and below 1 kev, the NDA⁹ nine-group shielded cross sections were used. The comparison between the computed integral ratios and the activation ratios is shown in Figure 3. The discrepancy between the measured and computed ratios near the outside boundary of the SP is qualitatively explained by the reflection of epithermal neutrons from the concrete walls back into the reactor. This reflection causes a relative increase in the near-thermal neutron flux close to the reactor surface which is not included in the calculations.

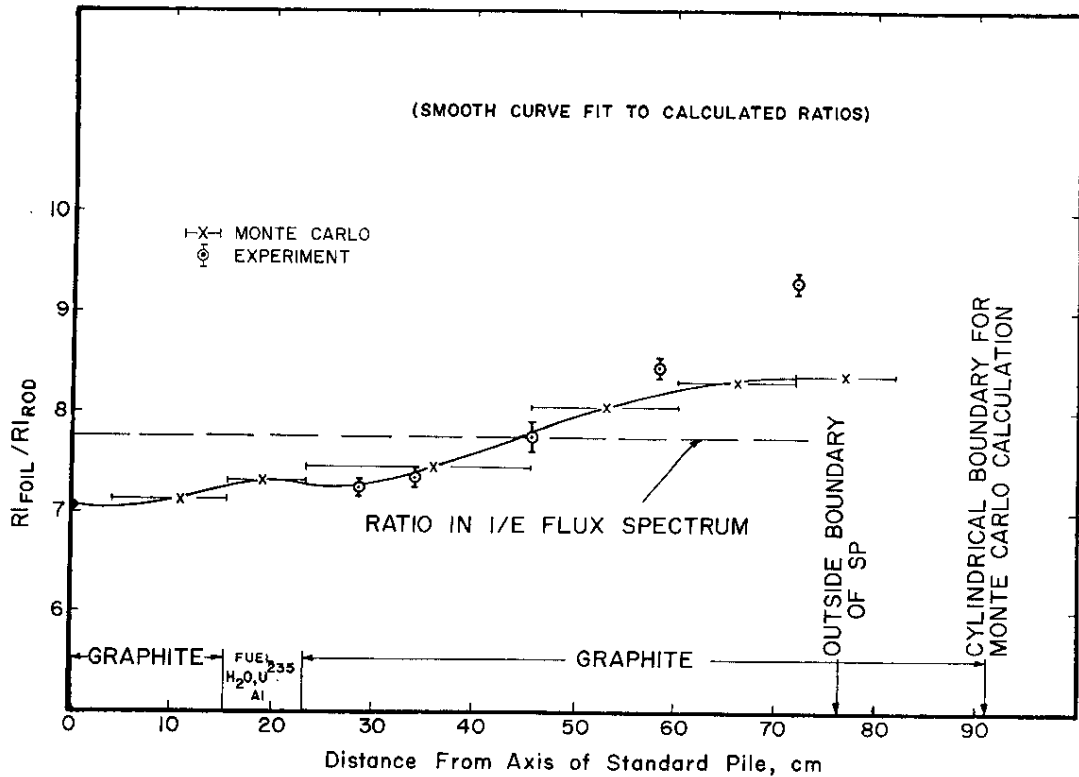


FIG. 3 MONTE CARLO COMPUTED RESONANCE INTEGRAL RATIOS COMPARED TO EXPERIMENTAL ACTIVATION RATIOS

Resonance integral measurements in an enriched uranium lattice in the D₂O-moderated Process Development Pile¹⁰ (PDP) at SRL further confirmed the Monte Carlo spectra calculations and the resonance capture integrals used in each lethargy interval to correct the measured resonance integrals to 1/E flux integrals. The Monte Carlo spectrum calculated for the test region in the PDP is depleted in the high energy component and differs markedly from the spectrum in the SP (Figure 4). The effective resonance integral was measured in both spectra using the same set of 0.940-, 0.750-, 0.500-, and 0.355-inch-diameter U-metal rods. The PDP and SP resonance integrals for U-metal agreed very well after they were corrected to 1/E flux integrals (Table I). The slightly lower resonance integrals from the PDP with the large rods are caused by diffusion depression of the flux in the adjacent fuel; this depression is not observed in the cavity at the center of the SP.

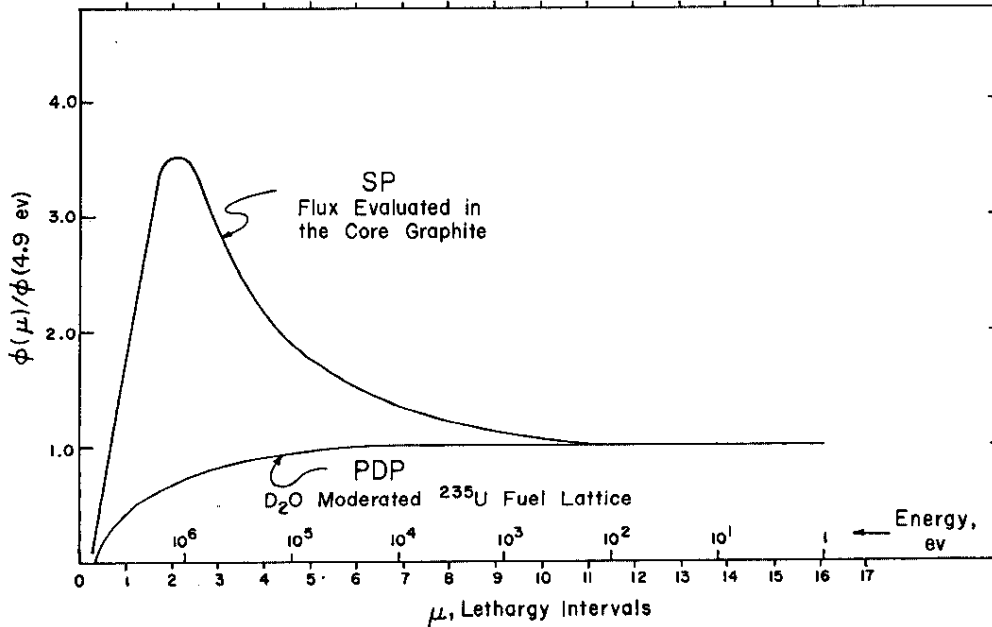


FIG. 4 MONTE CARLO COMPUTED EPITHERMAL FLUX SPECTRUM IN SP AND PDP

TABLE I

Uranium Metal Resonance Integrals Measured in SP and PDP

Rod Dia, inch	$\sqrt{S/M}$, cm/g ^{1/2}	RI		RI	
		No Spectrum Correction,* barns		With Spectrum Correction,* barns	
		SP	PDP	SP	PDP
0.940	0.298	13.72 ±0.11	11.63 ±0.11	12.06 ±0.24	11.57 ±0.13
0.750	0.333	14.98 ±0.11	13.15 ±0.15	13.31 ±0.22	13.03 ±0.16
0.500	0.408	16.79 ±0.08	15.29 ±0.18	15.07 ±0.20	15.17 ±0.19
0.355	0.485	19.11 ±0.13	17.50 ±0.18	17.44 ±0.23	17.35 ±0.19

* Resonance integrals shown in this table and the reported uncertainties are for the purpose of the comparison only and do not include corrections common to both measurements.

Counting Corrections

Deadtime

Deadtime corrections for window counting depend on pulses lying outside the window as well as those actually counted in the window. The standard two source method, utilizing depleted uranium source foils identical to the foils in the resonance integral measurements, was used to determine the counter deadtimes for the 90 to 116 kev window bias. The effective deadtime (based on window counts only) varied with time, reaching a minimum of 20 μ sec in 40 to 90 hours after irradiation.

Fission Products

The fission product activity contribution to the count rate in the 90 to 116 kev window had been investigated previously by comparing natural and depleted uranium activities⁵. This activity was also studied by observing the fission product activity deposited on aluminum catcher foils placed adjacent to the depleted uranium. The fission product contribution to the count rate was negligibly small (<0.2%) when the foils were counted in the interval from 2 to 4 days after irradiation.

Foil Size - Counter Efficiency

The foil radioactivity data were corrected for the variation in counter efficiency with foil diameter. Experimental efficiency factors were determined by comparing the measured specific activity of the 0.940-, 0.750-, and 0.355-inch-diameter foils with the specific activity of the 0.500-inch-diameter reference foils. The various sized foils had uniform source densities obtained by simultaneous irradiation in a uniform resonance flux. Auxiliary experiments using a 0.940-inch-diameter foil that had been irradiated in a rod section showed that the nonuniform radial distribution of activation in the foil did not significantly affect the magnitude of the correction.

Correction for $RI^{1/v}$ Component

The $1/v$ component of the resonance integral, if an isotropic $1/E$ flux is assumed incident on a $1/v$ detector, is given by

$$RI^{1/v} = 2F \sigma_0 \sqrt{E_0/E_{Cd}}$$

where

E_{Cd} = cadmium cutoff energy

σ_0 = absorption cross section at $E_0 = 0.0253$ ev

F = epithermal flux depression in the sample (self-shielding)

To determine E_{Cd} , the effective (equivalent slab geometry, isotropic flux incidence) cadmium thickness, δ , of the 32-mil cadmium covered cylindrical sample holder must first be determined. A sensitive method for determining δ was developed by measuring the ratio

$$\frac{RI_{\delta+Cd}^{Cu}}{RI_{\delta}^{Cu}}$$

where RI_{δ}^{Cu} = measured resonance integral of a copper foil located at the sample position in the holder

$RI_{\delta+Cd}^{Cu}$ = similarly measured resonance integral with a known thickness of cadmium added in slab geometry to each side of the copper foil*

An initial value of δ was estimated and a final value was determined by an iteration procedure using the measured ratio $RI_{\delta+Cd}^{Cu}/RI_{\delta}^{Cu}$ and a computed curve of RI_{Cd}^{Cu} versus cadmium thickness for the copper foil. This procedure gave a value of $\delta = 19$ mils, which corresponds to a cadmium cutoff energy of 0.55 ev. This value of δ was further confirmed by comparing the resonance activation of a copper foil irradiated at the sample position in the test apparatus with the activation of a similar foil enclosed in a 32-mil cadmium pill box in the same epithermal flux.

The $1/v$ component of the dilute resonance integral of U-metal was calculated to be 1.17 barns by using a cadmium cutoff energy of 0.55 ev. The epithermal depression factors given in Reference 5 were used to compute the $1/v$ component for the rod and packet resonance integrals.

Resonance Shielding Correction

The resonance activation of the reference foil is reduced because the rod section located in the adjacent sample holder shields the foil. (However, the reference foil does not appreciably shield the sample foil in the rod section.) The resonance

* The copper resonance integrals were corrected for the resonance shielding effect on the high energy copper resonances produced by the added cadmium. This effect was determined by suppressing the $1/v$ contribution to the copper resonance integral with boron absorber.

neutron flux at the reference foil is depleted by an amount dependent on the solid angle subtended by the rod section. A correction to the activation of 1.4% was computed for the rods of largest diameter (0.940 inch).

Finite Length Rod Correction

Resonance integrals for rods are generally determined for infinite length rods for which end effects are neglected. An investigation was undertaken to determine what effect a finite length rod would have on the activation of a foil at the rod midplane. A first order computation of the effect was derived by assuming that S/M is a valid parameter and that the resonance integral is given by the explicit relation $RI = A + B\sqrt{S/M}$ where A and B are constants. The resonance integral of a rod of radius R and length L is given by

$$RI(L) = A + B\sqrt{\frac{2 + \frac{2L}{R}}{\rho L}}$$

where ρ is the density of the rod. The resonance integral of the same rod with a thin foil of thickness ΔL inserted at the midplane is given by

$$RI(L + \Delta L) = A + B\sqrt{\frac{2 + \frac{2(L + \Delta L)}{R}}{\rho(L + \Delta L)}}$$

If the resonance integral of the rod is assumed to be unchanged by the insertion of the thin foil, the resonance integral of the combined foil and rod sections is the volume weighted average of the foil resonance integral and the rod resonance integral, i.e.,

$$RI(L + \Delta L) = \frac{L}{L + \Delta L} RI(L) + \frac{\Delta L}{L + \Delta L} RI(\Delta L)$$

The resonance integral of the foil is given by

$$RI(\Delta L) = A + B\sqrt{(S/M)_{\infty} \times F(R/L)}$$

where $F(R/L) = \frac{1 + R/2L}{\sqrt{1 + R/L}}$

$$(S/M)_{\infty} = 2/\rho R \text{ (The surface-to-mass ratio of an infinite length rod.)}$$

The validity of the assumption is improved as R/L is decreased (i.e., the length of the rod increased) or as $\Delta L/L$ is decreased (i.e., the foil thickness is reduced). The term $F(R/L)$ is a correction factor to convert the measured resonance integral of a finite length rod using a thin foil to the integral for the infinite length rod. In Figure 5 the computed function $F(R/L)$ is compared with experimental values of $F(R/L)$ obtained by measuring the resonance integral of various length 0.940- and 0.500-inch-diameter rods using 0.002-inch-thick foils. To make the comparison, the experimental results were normalized to the resonance integral of a 4-inch-long rod. A value of $A = 4.1$ barns was used. The data and the computations agree closely enough to confirm the use of computed correction factors for small values of R/L , and to justify the conclusion that a negligibly small correction factor is needed for the 4-inch-long rods. A numerical estimate of the effect of a finite length rod was also made for the 0.500-inch-diameter rod by numerical integration using a technique similar to that discussed in the next paragraph. As seen in Figure 5 the measured values agree somewhat better with the computed approximation than with the numerical estimate.

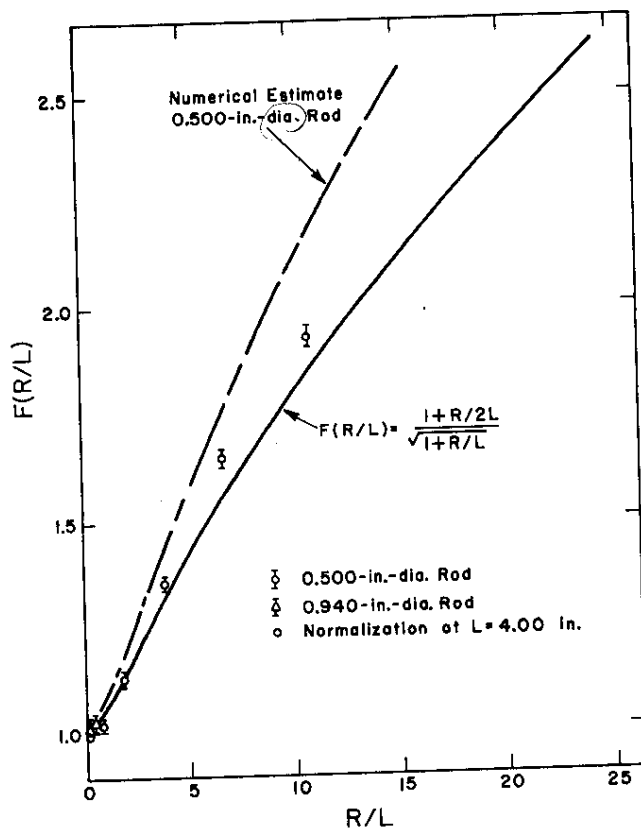
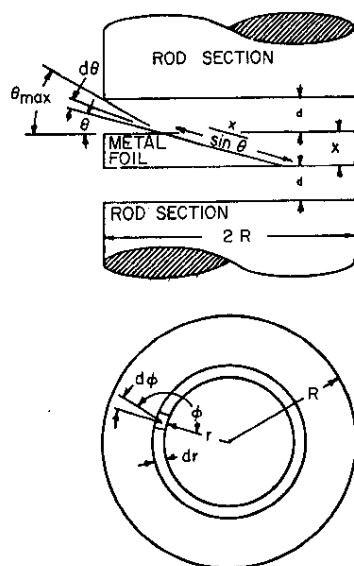


FIG. 5 COMPARISON OF COMPUTED AND MEASURED FINITE LENGTH ROD CORRECTIONS

Foil Gap Correction

A procedure was developed to compute the correction to the foil resonance integral to compensate for neutrons passing through small air gaps which remain after the measuring foil is inserted into the fuel rod. This procedure is indicated in Figure 6 where x is the foil thickness in mean free paths. In the equation at the bottom of the figure, ΔRI is the correction to the foil resonance integral, and $RI(r)$ is the radial distribution of the resonance integral in the rod. The integration is over all allowed angles and over the entire foil radius. The computations were simplified by assigning a single "average" resonance peak absorption cross section amplitude, $\sigma_{a_{max}}$, to all resonances. This average cross section is multiplied by the ^{238}U atom area density to give the effective nuclear thickness, x , of the metal foil in the diagram below. The "average" cross section, $\sigma_{a_{max}}$, was derived from the measured depression (Figure 10) for an isolated 0.002-inch foil. Doppler broadening is not explicitly included in the model, but its effect is implicitly included because of the experimental basis for the effective thickness.



$$\Delta RI = \frac{\frac{2}{R^2} \int_0^R [RI(x) - RI(r)] r dr \frac{1}{2\pi} \int_0^{2\pi} d\phi \frac{1}{\theta_{max}} \int_0^{\theta_{max}} \left(e^{-\frac{x}{2\sin\theta}} \right) I_0 \left(\frac{x}{2\sin\theta} \right) \sin\theta \cos\theta d\theta}{\frac{2}{\pi} \int_0^{\pi/2} \left(e^{-\frac{x}{2\sin\theta}} \right) I_0 \left(\frac{x}{2\sin\theta} \right) \sin\theta \cos\theta d\theta}$$

FIG. 6 GEOMETRICAL MODEL FOR COMPUTING EFFECT OF GAPS AT MEASURING FOILS ON RESONANCE INTEGRAL

The procedure was tested by introducing known gaps using aluminum spacers of various thicknesses adjacent to the foil in 0.940- and 0.355-inch-diameter rod measurements. The measured and computed gap corrections are compared in Figure 7. (The measurements have been slightly corrected for scattering and moderating in the aluminum to convert the results to those expected for a true air gap.) The data fit the computation even for the widest gaps. These measured corrections confirm small (~ 0.15 barn) corrections for the gaps (~ 0.0003 inch) in the actual rod experiments.

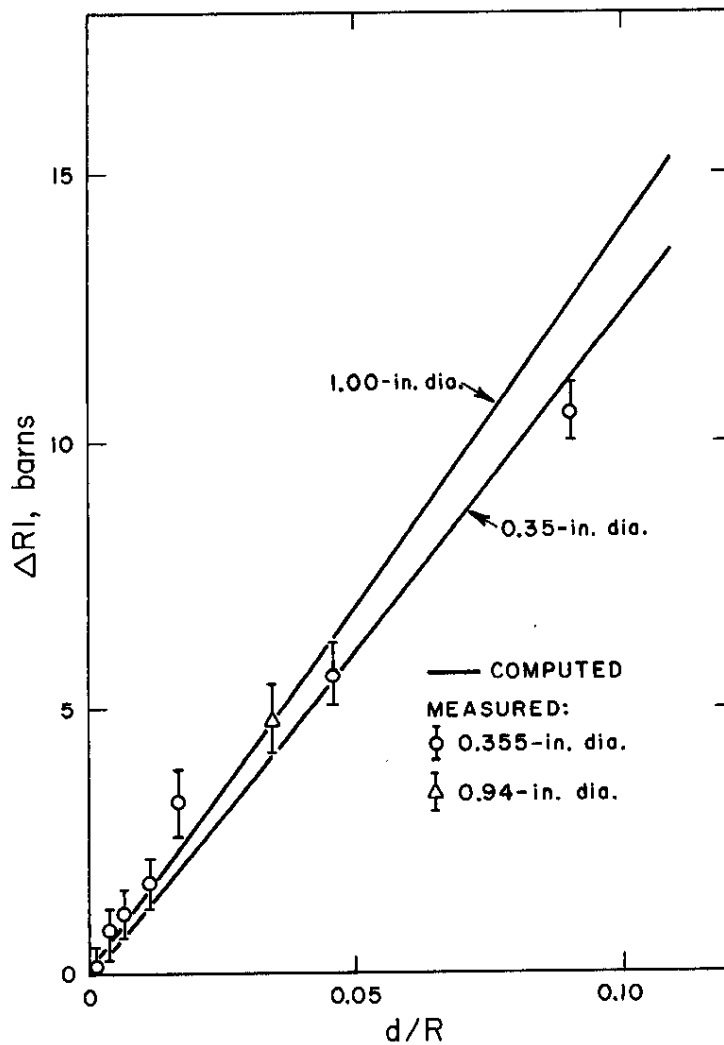


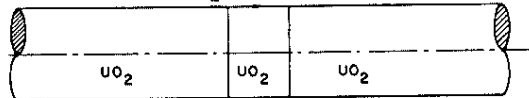
FIG. 7 COMPARISON OF COMPUTED AND MEASURED GAP CORRECTIONS

Correction for Use of Metal Foils in UO_2 and UC Rods

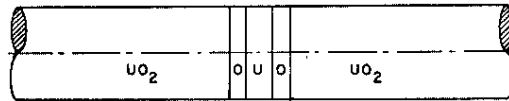
Resonance integrals for UO_2 and UC are hard to measure. Thin UO_2 or UC foils are difficult to fabricate. Thick foils necessitate large gamma-ray attenuation corrections. UO_2 or UC rods are difficult to dissolve and count. Experimentally, metal foils may be used in successively thinner layers to extrapolate to zero perturbation, but calculations show that the perturbation is strongly nonlinear as a function of foil thickness.

The models used to compute the perturbation of a U-metal foil in an UO_2 rod are shown in Figure 8. Figure 8A with a thin oxide segment is the desired model. In a hypothetical equivalent model (Figure 8B) this oxide segment is separated into metal and oxygen sections. The equivalent model is valid if the collision probability for neutrons in the oxygen layer is much smaller than unity,* and if the perimeter surface of the oxygen layer is small with respect to the rod cross-sectional area.† Finally, if these conditions are satisfied, a nearly equivalent foil model (Figure 8C) forms when the oxygen is removed. Thus, as a first approximation,

A IDEALIZED UO_2 ROD WITH UO_2 FOIL



B HYPOTHETICAL EQUIVALENT CONFIGURATION WITH U AND O_2 SEPARATED (SAME AVERAGE U AND O DENSITY)



C NEARLY EQUIVALENT CONDITION WITH O_2 REMOVED (SAME AVERAGE U DENSITY)

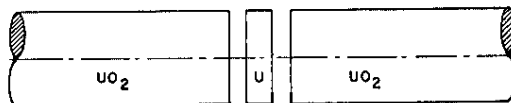


FIG. 8 MODELS USED TO DETERMINE URANIUM METAL FOIL PERTURBATION IN UO_2 RODS

* This probability has, as a corollary, the required physical condition that the probability for two successive collisions be negligible compared to the probability for only one.

† An auxiliary requirement is that the effect of crystalline binding on Doppler broadening be the same for U-metal as for UO_2 . Auxiliary experiments show the effects are closely the same for the rod sizes used.

the metal foil properly should have an air gap on either side. If no air gap is present, the effect of the metal foil in an oxide rod should be considered equivalent to a negative air gap. This consideration allows the computations for the air gap correction discussed earlier to be carried over directly. The effect of the energy exchange in the missing oxygen is computed separately in a conventional fashion.

Radial Misalignment of Foils

Radial misalignment of the foils relative to the solid rods was restricted to a maximum of 0.002 inch from the clearance between the rods and the aluminum holding tubes. Visual observations suggested that the actual misalignment was only a fraction of this amount. An experiment was designed to estimate maximum errors in the derived resonance integrals accurately due to such misalignment. To estimate these errors a set of 0.002-inch-thick depleted uranium foils were fabricated with diameters of 0.4950, 0.4975, 0.5000, 0.5025, and 0.5050 ± 0.0002 inch. The different foils were alternately positioned axially between the two 0.500-inch-diameter natural uranium metal rods, and irradiated under cadmium. The measured specific activities, corrected to the same neutron exposure, are compared in Figure 9 to the activity of the 0.5000-inch-diameter foil. The measured activity follows the expected shape, a nearly linear increase with radial misalignment for the oversize foils and an abrupt initial decrease for the undersize foils. The dashed curves of Figure 9 were used to derive by numerical integration the specific activity of an off-center 0.500-inch-diameter foil (solid curve Figure 9).

As expected, the activations lost due to indentation are nearly offset by those gained in the protruding section. The net effect of misalignment is to give measured resonance integrals that are lower than the correct values. The maximum error for the 0.500-inch-diameter rod is approximately 0.2%.

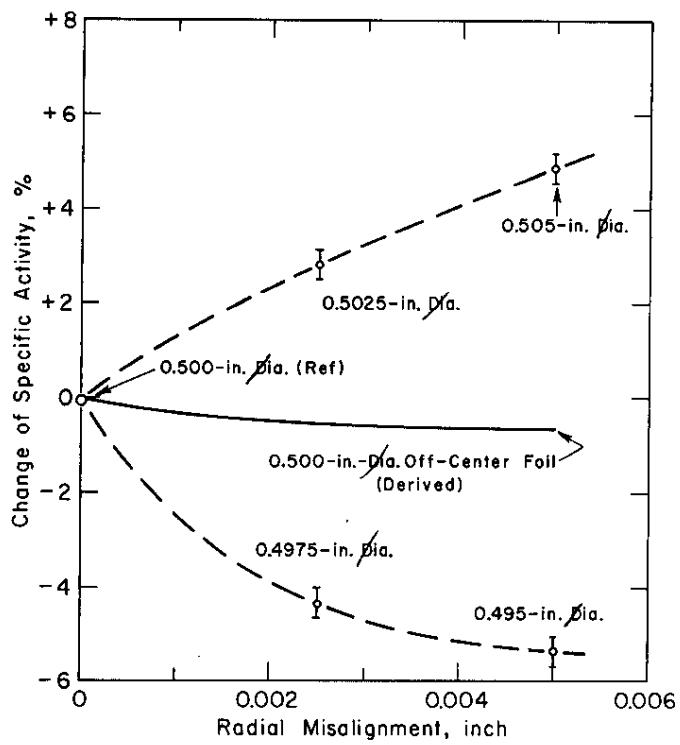


FIG. 9 EFFECT OF RADIAL MISALIGNMENT ON FOIL ACTIVITIES IN 0.500-IN. - DIAMETER URANIUM METAL BAR

RESULTS

The U-metal integral measurements are summarized in Tables II and III and are shown in Figure 10. (The foil data points represented by the open circles were obtained previously⁵ and are re-plotted here with spectrum $1/v$ corrections applied.) The U-metal rod and foil data closely fit the expression $3.50 + 25.1\sqrt{S/M_U}$ for $0.3 < \sqrt{S/M_U} < 6.0$. The 0.500-inch-diameter foil packet data fall below this fit for $0.48 < \sqrt{S/M_U} < 2.0$ which demonstrates a dependence on the detailed geometry. At higher $\sqrt{S/M}$ values the data fit calculations of the type proposed by Roe^{5,11} when normalized to the experimental infinite dilution integral of 277 barns. The uncertainty in the data points is approximately $\pm 3\%$.

TABLE II

Uranium Metal Resonance Integral Results - Rods

Rod Dia, inch	$\sqrt{S/M}$, $\text{cm/g}^{1/2}$ ($\rho=18.9$)	RI ^{Total} Uncorrected, barns	Corrections, barns				RI ^{1/v}	RI ^{Res} , barns
			Foil Size - Counter Efficiency	Resonance Shielding	Gap	1/E Flux		
0.940	0.298	13.07	+0.65	-0.18	-0.08	-1.65	-1.06	10.73
0.750	0.333	14.70	+0.28	-0.13	-0.10	-1.68	-1.08	11.99
0.500	0.408	16.79	0.00	-0.07	-0.15	-1.70	-1.10	13.77
0.355	0.485	19.11	0.00	-0.04	-0.20	-1.73	-1.12	16.02

TABLE III

Uranium Metal Resonance Integral Results - 0.500-inch-Diameter Foil Packets

$\sqrt{S/M}$, $\text{cm/g}^{1/2}$	RI ^{Total} Uncorrected, barns	1/E Flux Correction, barns	RI ^{1/v} Correction, barns	RI ^{Res} , barns
4.46	119.0	-2.17	-1.17	115.7
3.18	86.90	-2.15	-1.17	83.58
2.04	56.75	-2.13	-1.17	53.45
2.03	57.15	-2.13	-1.17	53.85
1.47	42.73	-2.08	-1.17	39.50
1.20	35.63	-2.03	-1.16	32.44
0.942	29.26	-1.95	-1.15	26.16
0.725	23.27	-1.85	-1.14	20.28
0.594	20.48	-1.77	-1.12	17.59
0.537	19.60	-1.75	-1.11	16.74
0.480	18.06	-1.73	-1.10	15.23

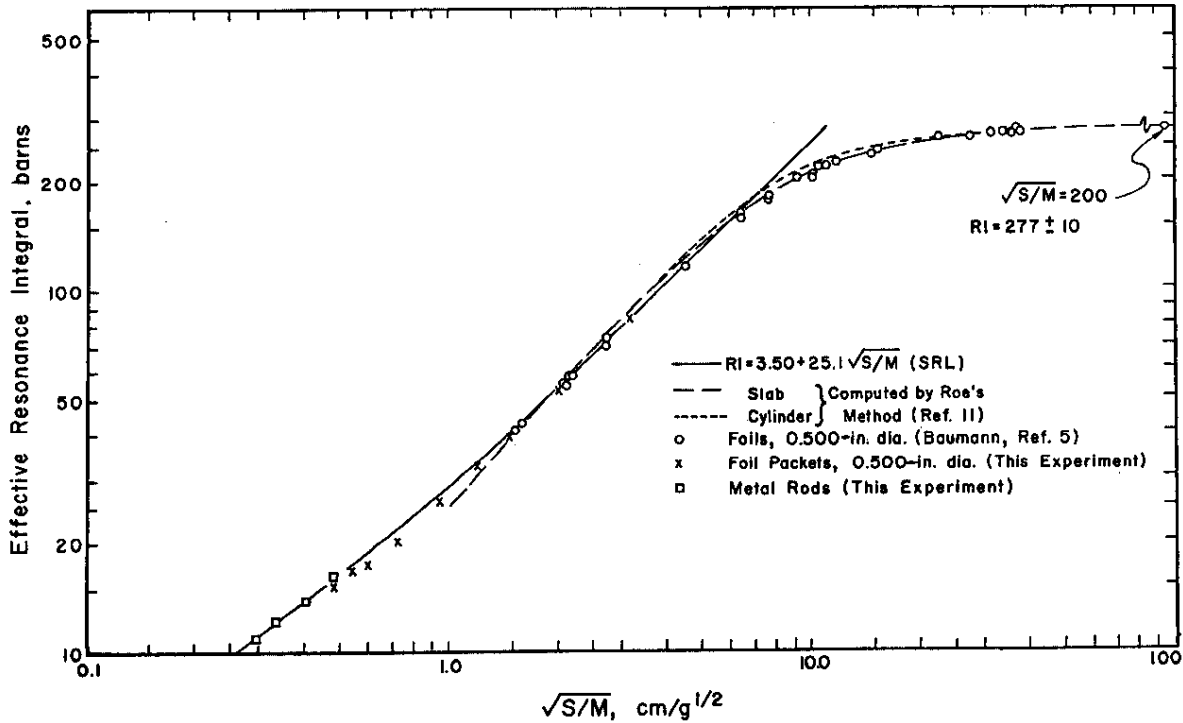


FIG. 10 EFFECTIVE RESONANCE INTEGRAL FOR URANIUM METAL

The UO_2 rod integral measurements are summarized in Table IV and are shown in Figure 11. The data fit the expression $5.25 + 24.35 \sqrt{S/M} UO_2$. The uncertainty in the data points is approximately $\pm 3\%$. The equivalence theorem¹² has been used to compare the oxide results with the metal. The comparison was made by use of the expression

$$\left(\frac{S}{M}\right)_U^{Eq} = \left(\frac{S}{M}^{238}\right)_{UO_2} + 0.0101 \sigma_m \times f(A)$$

where σ_m is the potential scattering cross section of oxygen in barns per ^{238}U atom in the oxide ($\sigma_s(O_2) = 7.6$ barns) and $f(A)$ is a factor that corrects for the scattering effectiveness of the oxygen moderator in removing neutrons from the ^{238}U resonance. The equivalence theorem comparisons are shown in Figure 11. The 0.94-inch-diameter rod data is best fit by $f(A) = 0.4$, but the best overall agreement is with $f(A) = 0.3$. These values compare to a computed factor of 0.55¹³ and a negative value obtained from a similar analysis of the Bettis experimental results¹⁴.

TABLE IV

Uranium Oxide Resonance Integral Results - Rods

Rod Dia, inch	$\sqrt{S/M},$ cm/g ^{1/2} ($\rho=10.3$)	RI ^{Total} Uncorrected, barns	Corrections, barns						RI ^{Res} , barns
			Foil Size - Counter Efficiency	Resonance Shielding	Gap	Metal Foil	1/E Flux	RI ^{1/v}	
0.940	0.403	17.00	+0.76	-0.23	-0.08	+0.31	-1.59	-1.10	15.03
0.750	0.452	18.58	+0.36	-0.16	-0.10	+0.38	-1.61	-1.12	16.31
0.500	0.553	21.22	0.00	-0.08	-0.15	+0.54	-1.65	-1.13	18.75
0.355	0.656	23.47	0.00	-0.05	-0.20	+0.74	-1.69	-1.14	21.13

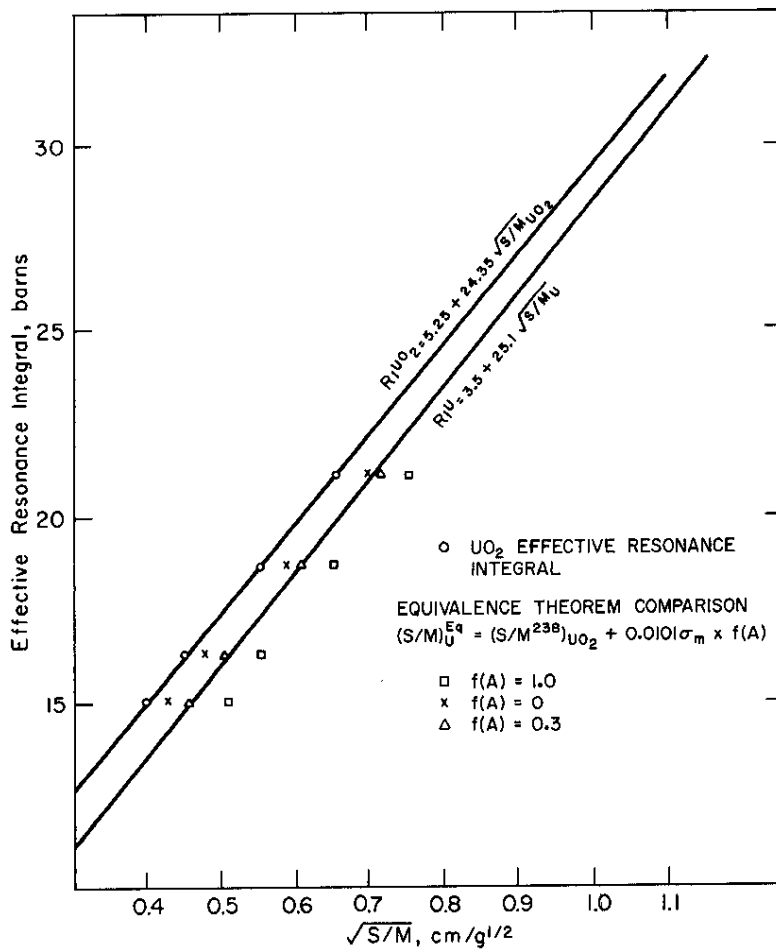


FIG. 11 EFFECTIVE RESONANCE INTEGRALS FOR UO₂ AND EQUIVALENCE THEOREM COMPARISON

The UC rod integral measurements are summarized in Table V and are shown in Figure 12. The uncertainty in the data points is approximately $\pm 4\%$. The data fit the expression $5.05 + 26.2 \sqrt{S/M_{UC}}$. The equivalence theorem comparison shows that a value of $f(A) > 1.0$ is required for UC to agree with the metal.

TABLE V
Uranium Carbide Resonance Integral Results - Rods

Rod Dia, inch	$\sqrt{S/M}$, cm/g ^{1/2}	ρ , g/m	RI ^{Total} Uncorrected, barns	Corrections, barns								RI ^{Res} , barns
				Foil Size - Counter Efficiency	Resonance Shielding	Gap	Metal Foil	1/E Flux	RI ^{1/v}	To ∞ Length		
0.940	0.354	13.40	16.54	+0.53	-0.23	-0.08	+0.19	-1.59	-1.10	-0.07	14.19	
0.750	0.396	13.39	17.97	+0.33	-0.16	-0.10	+0.24	-1.61	-1.12	-0.07	15.48	
0.500	0.483	13.52	20.34	0.00	-0.08	-0.15	+0.34	-1.65	-1.13	0.00	17.67	
0.355	0.574	13.47	22.80	0.00	-0.05	-0.20	+0.46	-1.69	-1.14	0.00	20.18	

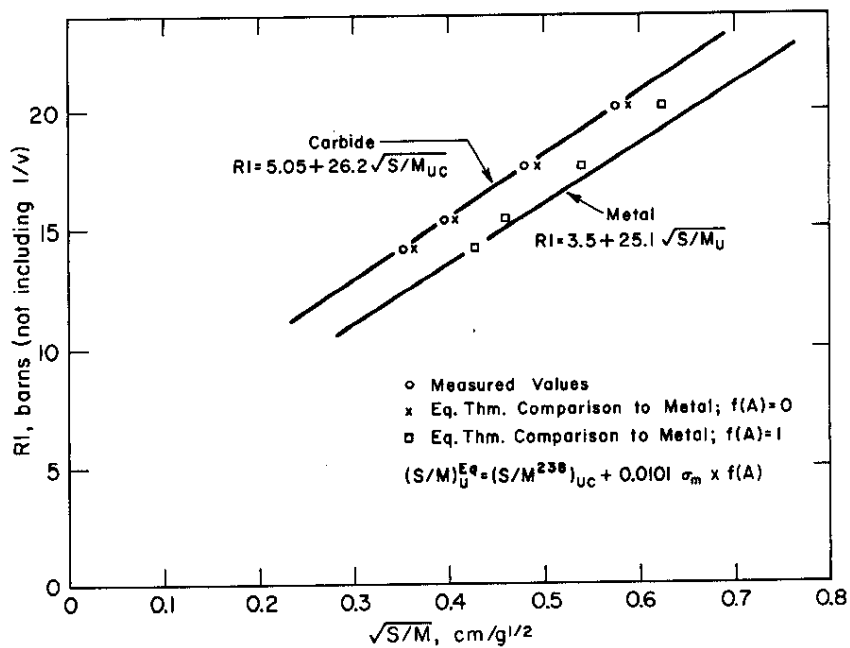


FIG. 12 MEASURED URANIUM CARBIDE RESONANCE INTEGRALS AND EQUIVALENCE THEOREM COMPARISON TO URANIUM METAL

REFERENCES

1. E. Hellstrand and G. Lundgren. "The Resonance Integral for Uranium Metal and Oxide." Nucl. Sci. Eng. 12, 435 (1962).
2. J. Hardy, Jr., G. G. Smith, and D. Klein. "The Effective Resonance Capture Integrals of Uranium Metal and UO_2 Rods." Nucl. Sci. Eng. 14, 358 (1962).
3. K. Jirlow and E. Johansson. "The Resonance Integral of Gold." J. Nucl. Energy Part A: Reactor Science 11, 101 (1960).
4. R. C. Axtmann, et al. Initial Operation of the Standard Pile. USAEC Report DP-32, E. I. du Pont de Nemours and Co., Savannah River Laboratory, Aiken, S. C. (1953).
5. N. P. Baumann. Resonance Integrals and Self-Shielding Factors for Detector Foils. USAEC Report DP-817, E. I. du Pont de Nemours and Co., Savannah River Laboratory, Aiken, S. C. (1963).
6. W. V. Baxter. A Monte Carlo Code for the Transport of Neutrons. USAEC Report DP-446, E. I. du Pont de Nemours and Co., Savannah River Laboratory, Aiken, S. C. (1959).
7. N. D. Goldberg, S. F. Mughabghab, S. N. Purohit, B. A. Magurno, and V. A. May. Neutron Cross Sections. USAEC Report BNL-325. Suppl. No. 2, 2nd Ed. Vol. I and II, Brookhaven National Laboratory, Upton, N. Y. (1966).
8. A. R. Vernon. "Calculation of the Effective Resonance Integral of ^{238}U ." Nucl. Sci. Eng. 7, 252 (1960).
9. J. Agresto, et al. A Method for Calculating the Reactivity of Simple D_2O -Moderated Natural Uranium Lattices. USAEC Report NDA 2131-20, Nuclear Development Corporation of America, White Plains, N. Y. (1960).
10. A. E. Dunklee. PDP Heavy Water System. USAEC Report DP-567, E. I. du Pont de Nemours and Co., Savannah River Laboratory, Aiken, S. C. (1961).
11. G. M. Roe. The Absorption of Neutrons in Doppler Broadened Resonances. USAEC Report KAPL-1241, Knolls Atomic Power Laboratory, Schenectady, N. Y. (1954).
12. J. Chernick and R. Vernon. "Some Refinements in the Calculations of Resonance Integrals." Nucl. Sci. Eng. 4, 607 (1958).

13. M. L. Levine. "Resonance Integral Calculations for U^{238} Lattices." Nucl. Sci. Eng. 16, 271 (1963).
14. J. Hardy, Jr., D. Klein, and G. G. Smith. "Some Experimental Results Pertinent to Equivalence Relations for Effective Resonance Integrals." Nucl. Sci. Eng. 14, 366 (1962).